Available online at www.sciencedirect.com
ScienceDirect
Polymer 48 (2007) 5088–5097
polymer
www.elsevier.com/locate/polymer

Crystalline structure of poly(hexamethylene succinate) and single crystal degradation studies

Sebastià Gestí, María Teresa Casas, Jordi Puiggalí*

Departament d'Enginyeria Química, Universitat Politècnica de Catalunya, Av. Diagonal 647, E-08028 Barcelona, Spain

Received 20 March 2007; received in revised form 12 June 2007; accepted 18 June 2007
Available online 28 June 2007

Abstract

The morphology of solution grown single crystals of poly(hexamethylene succinate) (PE 6 4) was investigated using dilute alcohol or diol solutions by isothermal crystallization. Increasing temperatures changed the morphology of truncated rhombic crystals, which became lenticular crystals. Spiral growths and multilayered crystals as well as characteristic striations which mainly form in the {110} sectors were often observed. A regular folding surface was found by using polyethylene decoration techniques. Lamellar crystals were easily degraded with different lipases. A preferential enzymatic attack was observed to occur on the crystal edges, giving rise in some cases to highly irregular borders with a fringed texture.

Lamellae gave rise to well resolved electron diffraction patterns that allowed the main packing characteristics to be determined. Fiber X-ray diffraction patterns indicate a quasi planar zig-zag conformation and a large unit cell containing eight molecular segments. This cell could not be deduced from the typical *hk*0 electron diffraction pattern but could be assessed from the patterns of tilted specimens.

Simulation of electron diffraction patterns indicates that molecular segments are arranged with setting angles close to ±46° or ±226°. In addition, neighbouring chains along both *a*- and *b*-axis have setting angles differing by 180° in order to justify the deduced cell dimensions.

Keywords: Polyester; X-ray diffraction; Electron microscopy

1. Introduction

A large number of polymers whose main chains can be degraded usefully have recently been proposed [1,2]. Among these polymers, aliphatic polyesters are receiving special attention because they are all more or less sensitive to hydrolytic degradation [3,4]. However, only some of these polyesters are enzymatically degradable and an even smaller number are bio recyclable [5].

Interest in polyesters derived from diols and dicarboxylic acids has increased since the commercialization of poly(butylene succinate) [6] (PBS). This is a biodegradable synthetic aliphatic polyester [7] that exhibits excellent mechanical properties. PBS is generally blended with other compounds, such as starch and adipate copolymers to make its production economical [8,9].

Structural studies on poly(alkylene dicarboxylate)s are relatively scarce and mainly concern commercial poly(butylene succinate) and poly(butylene adipate) samples. Kink conformations based on a pair of *gauche* bonds with opposite signs have been proposed for some ethylene glycol, succinic and adipic acid derivatives [10–12]. However, a quasi all-*trans* conformation has usually been found, in particular when the methylene content of both diol and dicarboxylic units is high [13].

Electron diffraction patterns of polyesters with the zig-zag conformation indicate that the unit cells projected along the chain axis are rectangular, the parameters being close to $a = 0.500–0.504$ nm, and $b = 0.73–0.75$ nm. These values are similar to those reported for polyethylene (considering the

* Corresponding author. Tel.: +34 93 4016684; fax: +34 93 4010978.
E-mail address: jordi.puiggali@upc.es (J. Puiggalí).

0032-3861/$ - see front matter © 2007 Elsevier Ltd. All rights reserved.
doi:10.1016/j.polymer.2007.06.057

change in the axes definition) and correspond to a cell content of two molecular segments. However, recent works on some 1,4-butanediol [14] and 1,6-hexanediol [15] derivatives have revealed the existence of unit cells where the *b*-axis parameter is doubled. The structure becomes more complex because the two neighbouring molecules along the *b*-axis are only equivalent in chain axis projection. Simulation of X-ray diffraction data indicates that these two unit cell molecules are shifted along the chain axis, and also that their setting angles differ by 180°. Poly(hexamethylene dodecanoate) [15] is a clear example of a polymer with this kind of structure, whereas the unit cell of poly(hexamethylene adipate) [16] also shows an increase in the *a*-axis parameter. Both polymers are defined by orthorhombic unit cells, although the indicated shifts reduce the symmetry expected for the smaller cells. In this way, a monoclinic space group has been postulated for poly(hexamethylene adipate) [16]. In the present work, we continue with the study of the succinate derivative in order to complete the structural and morphologic data on the series of polymers based on 1,6-hexanediol. The potential use of these polyesters may also be interesting because this diol is a valuable intermediate for the chemical industry.

2. Experimental section

Polyester 6 4 was synthesized from succinic acid using an excess of 1,6-hexanediol (molar ratio 2.2/1) by thermal polycondensation at 160 °C in a nitrogen atmosphere for 4 h and then in vacuum at 180 °C for 24 h. Titanium tetrabutoxide was used as a catalyst. The polymer was dissolved in chloroform and precipitated with ethyl ether. The polymerization yield was 75%. An intrinsic viscosity of 0.81 dL/g was measured with a Cannon-Ubbelhode microviscometer in dichloroacetic acid solutions at 25 ± 0.1 °C. In addition, the molecular weight distribution was determined by size exclusion chromatography (SEC) using a liquid chromatograph (Shimadzu, model LC-8A) equipped with an Empower computer program (Waters). The average molecular weights were calculated using poly(methyl methacrylate) standards. A PL HFIPgel column (Polymer Lab) and a refractive index detector (Shimadzu RID-10A) were used. The polymer was dissolved and eluted in hexafluoroisopropanol at a flow rate of 0.5 mL/min (injected volume: 100 μL, sample concentration: 1.5 mg/mL). Values of 13 900, 37 900 and 2.7 were determined for M_n, M_w and the polydispersity index, respectively.

Isothermal crystallizations were carried out in the 10–50 °C range from dilute solutions (0.005% w/v) in alcohols such as *n*-butanol, and diols like 2-methyl-2,4-pentanediol. A drop of the solution was placed on a carbon-coated grid, and the solvent was allowed to evaporate in order to avoid a crystal breakage that could occur when very thin crystals are separated by centrifugation. The crystals were finally shadowed with Pt–carbon at an angle of 15° for bright field observations. Polymer decoration was achieved by evaporating polyethylene onto the surface of single crystals, as described by Wittmann and Lotz [17].

A Philips Tecnai 10 electron microscope was used and operated at 80 and 100 kV for bright field and electron diffraction modes, respectively. Bright field micrographs were taken with a SIS MegaView II digital camera. Selected area electron diffraction patterns were recorded on Kodak Tri-X films. The patterns were internally calibrated with gold ($d_{111} = 0.235$ nm). Electron diffraction patterns were digitized and the intensity of reflections determined by means of the ELD program [18]. This also allowed the intensity of saturated reflections to be estimated by a shape fitting procedure. If a reflection is saturated, the central part of the spot is useless. However, its tail will not be saturated and so it can be compared to the tail of a Gaussian type function. A curve fitting algorithm is used by the program to estimate what the reflection intensity would be if the spot were not saturated. Correction for non-linearity of the photographic film was made by considering a calibration strip of known optical densities.

Degradation of polyester 6 4 single crystals was performed with lipases from *Rhizopus arrhizus* (1500 units/mg) and *Pseudomonas cepacia* (40 units/mg). Lamellar crystals, obtained by crystallization in *n*-butanol at 30 °C, were deposited on carbon-coated gold grids. These grids were immersed on 20 μL of a pH 7.0 buffered medium of 50 mM tris–HCl containing the enzyme (0.13 mg/mL) at a constant temperature of 37 °C. After different exposure times, the grids were repeatedly washed with distilled water and ethanol, and finally shadowed with Pt–carbon. Controls without enzyme were also run.

AFM examination of single crystals was performed with a Digital Instruments Nanoscope IV under tapping mode using silicon tips with a resonance frequency of 25 kHz and a spring constant of 0.4 N/m. Both height and phase images were recorded simultaneously.

X-ray diagrams were recorded under vacuum at room temperature using calcite as a calibration standard. A modified Statton camera (W. R. Warhus, Wilmington, DE, USA) with Ni filtered Cu radiation of wavelength 0.1542 nm was used. Fibers were prepared from the melt and annealed under stress at 37 °C.

The experimental fiber density was calculated by the flotation method using ethanol and carbon tetrachloride as solvents. A value of 1.17 g/mL was obtained.

Structural modeling was carried out by means of the diffraction software package of the Cerius^2 (Accelrys Inc.) [19] computer program. All calculations were run on a Silicon Graphics Octane Workstation.

3. Results and discussion

3.1. Solution grown single crystals

Isothermal crystallization of polyester 6 4 in dilute alcohol solutions gives rise to lamellar single crystals with a morphology that clearly depends on the crystallization temperature (Fig. 1). The axial ratio and lateral habit change similarly as previously reported for polyester 6 6 [16], and as well

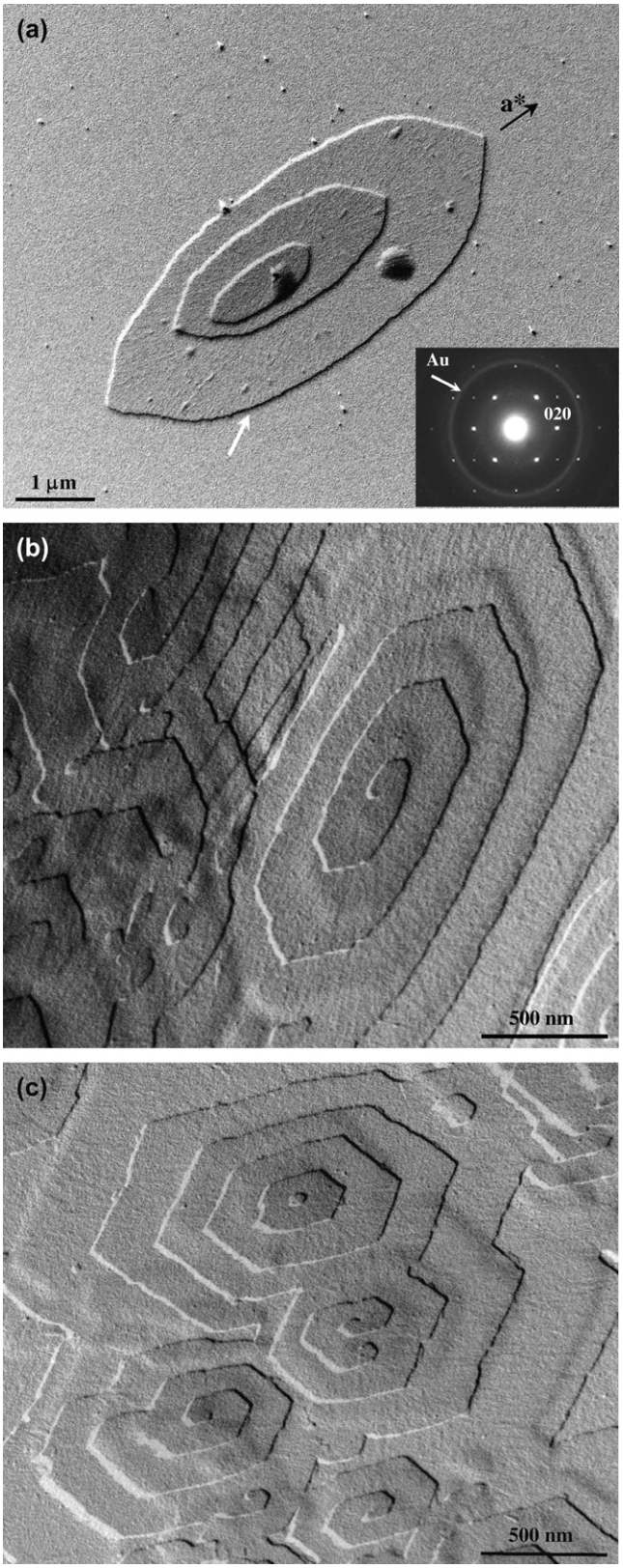

Fig. 1. Electron micrographs of polyester 6 4 lamellar crystals obtained from dilute *n*-butanol solutions at 50 °C (a), 45 °C (b) and 30 °C (c) showing a high dependence on between morphology and crystallization temperatures. Thus, crystals obtained at the highest temperature show a lenticular morphology with curved {010} growth faces (see white arrow). All crystals are characterized by the presence of striations which mainly form in the {110} sectors. Inset shows a characteristic electron diffraction pattern with a ring corresponding to the gold used for calibration. An index is given for the smallest rectangular unit cell defined by the electron diffraction pattern. The *a**-axis is indicated in (a) in order to clarify the orientation of the electron diffraction pattern respect to morphology.

established for polyethylene [20]. Therefore, the increase in the ester/methylene group ratio does not dramatically vary the main morphological features described for polyethylene whose lateral habit changes from rhombic lamellae at low crystallization temperatures T_c [21–23] to lenticular lamellae at the highest T_c [24]. Of course, the lower melting point of polyester 6 4 requires crystallizations to be performed at a lower temperature range than polyethylene.

Lenticular crystals of polyester 6 4 can be easily obtained from different solvents such as *n*-butanol at temperatures close to 50 °C. Their electron diffraction patterns define a rectangular unit cell whose parameters ($a = 0.503$ nm and $b = 0.732$ nm) are close to those found in aliphatic polyesters and polyethylene. The patterns allow a molecular chain orientation perpendicular to the crystal basal plane to be postulated. Consequently, a molecular folding can be inferred by considering the molecular weight of the sample and the reduced lamellar thickness deduced from the shadow of the crystals. It can be also noted that crystals become elongated in the *a*-crystallographic axis direction when correlation between bright field images and electron diffraction patterns is taken into account. The crystals shown in Fig. 1(a) are also characterized by a pronounced curvature affecting the {010} faces while the {110} faces are practically straight (faceted). Note that these crystallographic features are identical to those found in polyethylene since the *a*- and *b*-axis are inversely defined.

Rounded crystal habits of polyethylene have been explained by Sadler [25], who used a rough-surface theory of crystal growth. This implies a statistical attachment of stems to rough surfaces that prevents development of crystallographic faceting. Other approaches [26–28] resting on Frank's equations [29] regarding crystal growth by secondary nucleation have been formulated in order to qualitatively explain the curvature of the corresponding faces in polyethylene. Curvature occurs when the average propagation distance is no greater than several stem widths. In this way, crystal growth becomes intermediate between nucleated and rough-surface type.

At lower temperatures (e.g. 35 °C) polyester crystals show a truncated lozenge morphology with a high aspect ratio. Note that a slight curvature of the {010} faces can still be detected in the crystals depicted in Fig. 1(b). When the crystallization temperature decreases to 30 °C, a regular polygonal habit is observed and the aspect ratio of the truncated crystals decreases again (Fig. 1(c)). At this temperature, the l_a/l_b ratio between the lengths of the crystals in the [100] and [010] directions becomes close to 1.8. The morphology of the observed truncated single crystals is also characterized by angles of 108° and 127°, between the two {110}, and the {110} and {010} growth faces, respectively, which are in full agreement

with those values calculated from the dimensions of the planar unit cell (110.0°, 124.5°). This faceted habit indicates that {110} and {010} growth at moderate supercooling can be safely regarded as nucleation controlled.

Left and right spiral dislocations are the most important defect observed in the formed crystals. Both types of dislocations are observed in a similar proportion since the studied polyester has a non-chiral molecular conformation. In addition, multilayered crystals, whose terraces can be interpreted as a combination of the two kinds of screw dislocations, are also detected. The indicated dislocations have an amplitude defined by a Burgers vector equal to the lamellar thickness which includes the crystalline core and both folding surfaces. Although crystallographic coherence may be forbidden between successive layers, the terraces of the studied polyester do not show rotation and appear in a crystallographic register. In fact, a rotation pattern has always been associated with a pyramidal habit of the basal crystal [30].

Crystals with a practically hexagonal habit can only be obtained at a high supercooling and using a different solvents like 2-methyl-2,4-pentanediol (Fig. 2). However, at low temperature crystallization is difficult and some poorly crystallized material with a rounded morphology can be clearly detected. These small crystalline globs are indicative of phase separation and appear admixed with the single crystals produced in the dilute phase. No lozenge crystals without development of the truncated {010} faces could be obtained since, at the required temperature, the solution tends to separate into two liquid phases because of poor solvent characteristics.

Polyester 6 4 single crystals frequently develop striations independently of the solvent used in the crystallization (e.g. Figs. 1 and 2 for (*n*-butanol) and (2-methyl-2,4-pentanediol), respectively). Striations mainly appear in the {110} sectors, and can consequently be well detected in the crystallizations performed at high supercoolings where lamellae show well developed {110} sectors. In fact, striations are clearly enhanced in the crystals shown in Fig. 2, where badly crystallized material also exists, as above explained.

The AFM height image and line profile data of lamellar crystals obtained at 35 °C indicate a planar surface with a fairly constant monolamellar thickness close to 9.0 nm (Fig. 3). However, the surface becomes rough as a consequence of the previously mentioned striations whose height varies largely depending on the crystal and the zone. Thus, the range usually extends over 0.7–2.5 nm.

Striations seem to develop in a regular way and, in particular seem to be parallel oriented in the [100] crystallographic direction or with a slight deviation in a radial direction. No perpendicular orientation to the growth faces is detected. Striations have been reported for different polyesters (e.g. polyester 4 6 [31] polyester 12 10 [13], poly-β-propiolactone [32], poly-ε-caprolactone [33] and polyester 6 6 [16]), and several explanations for them have been provided. For

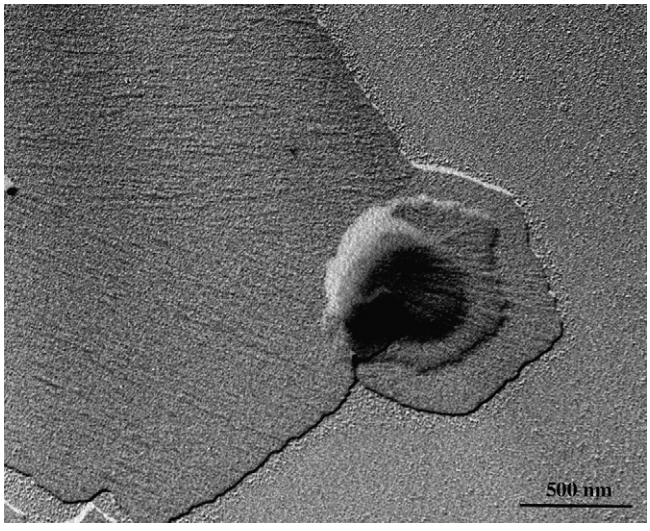

Fig. 2. Electron micrograph of polyester 6 4 lamellar crystals obtained from a dilute 2-methyl-2,4-pentanediol solution at 30 °C. The observed crystal growth in the [100] direction is lower than that found for the lamellae depicted in Fig. 1. Smaller crystals tend to exhibit a hexagonal morphology although rounded globs can also be detected as a consequence of poor solvent characteristics. Striations are clearly noticeable and appear with a practically radial direction.

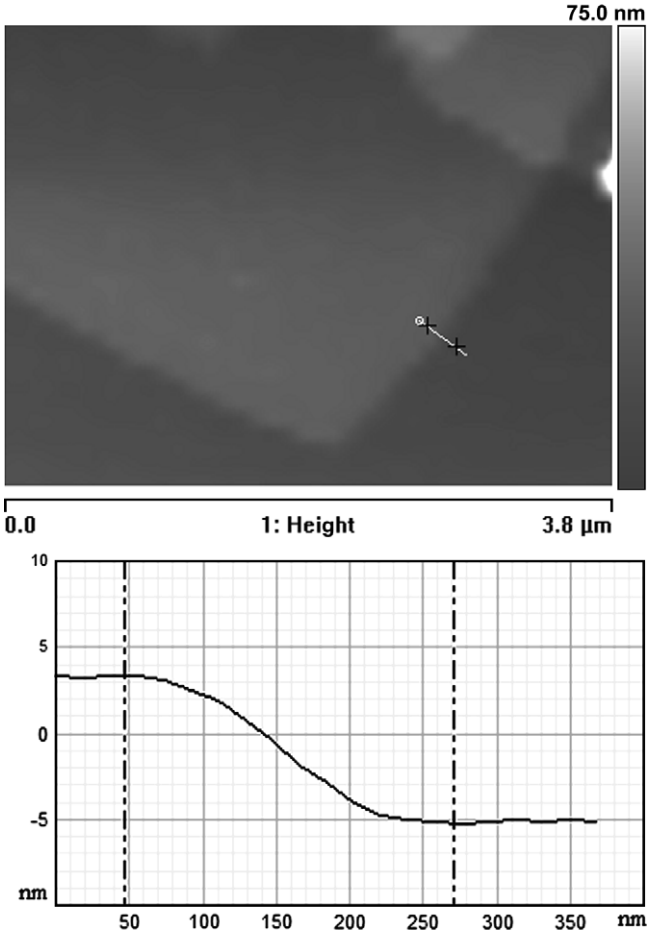

Fig. 3. Atomic Force Microscope height images and corresponding thickness profiles of a single polyester 6 4 lamellar crystal obtained from a dilute 2-methyl-2,4-pentanediol solution at 35 °C. In this case, a lamella without striations has been selected in order to measure lamellar thickness more accurately.

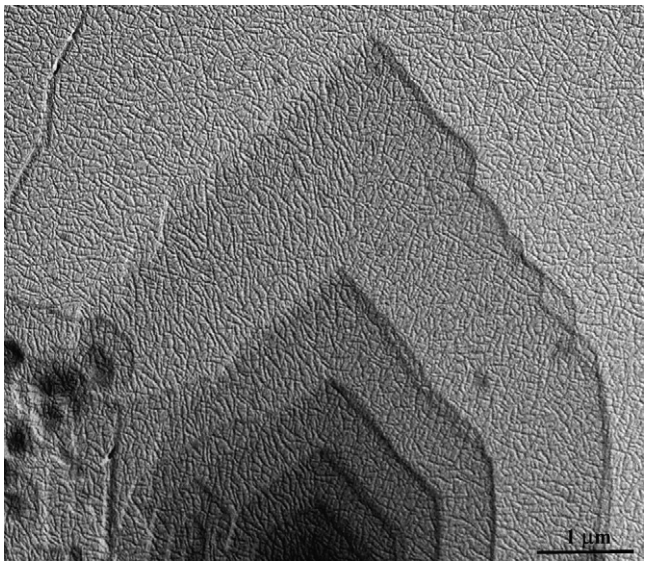

Fig. 4. Polyethylene decoration of polyester 6 4 lamellar crystals obtained from 2-methyl-2,4-pentanediol at 35 °C.

example, their origin has been based on the existence of different chain-packing states in the crystal, on a twinning involving a small chain axis shear of molecular chains or on an aggregation of microcrystals. For this reason, degradation studies on poly(ε-caprolactone) lamellar crystals suggest a possible microcrystal organization [33]. Large rhombic crystals constituted by aggregates of small lath-like lamellae have also been observed in some polyamides [34].

Polyethylene decoration highlights the sectorization of single crystals and also supports a regular folding mechanism (Fig. 4). The decorating rods were preferentially placed perpendicular to the {110} and {010} growth faces, suggesting that the chain folding is parallel to the indicated planes. In fact, folds may take place between neighbouring chains in both [110] and [100] directions since molecular chains are adirectional. This feature is not feasible in some directional polyesters such as hydroxyacid derivatives since an antiparallel molecular chain arrangement is only established in the [110] diagonal directions of their unit cells [35]. Observations are consistent with the characteristic polymer crystal growth occurring normal to the fold planes. These stack successively on each other as they are nucleated and fill out with folded chains.

3.2. Enzymatic degradation of lamellar crystals

Fig. 5(a) shows that degradation of polyester 6 4 clearly takes place under the attack of a lipase from *R. arrhizus*. A lamella with a regular morphology can be well distinguished in the micrograph since it was deposited under the other lamellae, and was consequently protected from the enzymatic attack, whereas the other two lamellae that appear in the micrograph show a similar type of degradation. The attack at the {110} sectors seems to begin at the edges of the crystals and progresses towards the center of the lamellae following

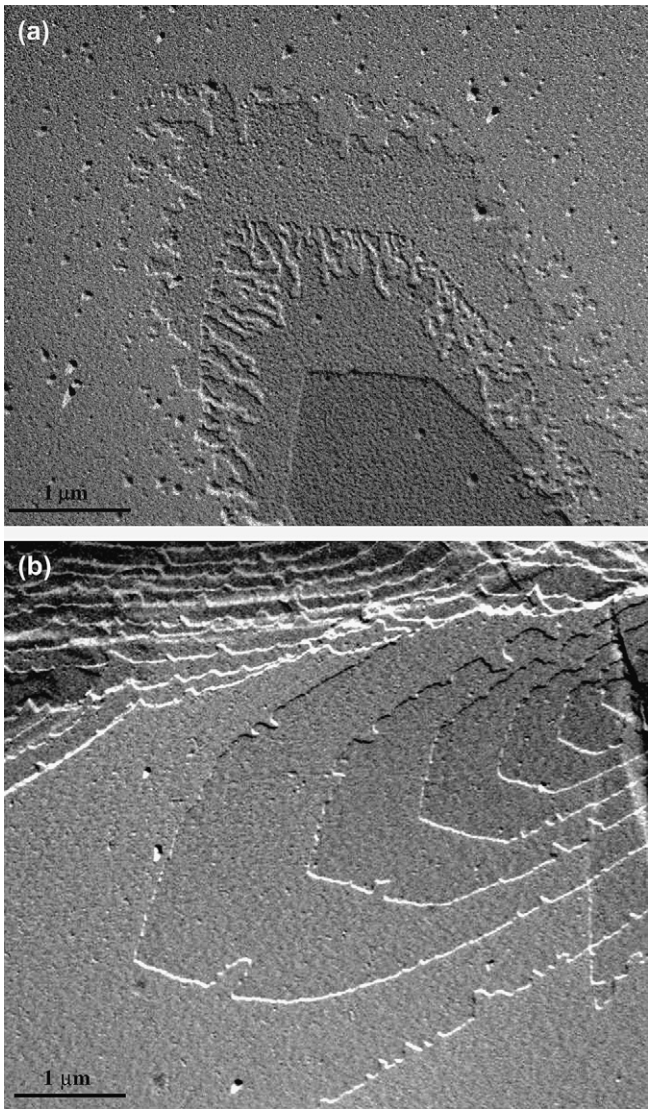

Fig. 5. Electron micrographs of polyester 6 4 lamellar crystals obtained from dilute *n*-butanol solutions at 30 °C and exposed to a lipase from *Rhizopus arrhizus* (a) and *Pseudomonas cepacia* (b) media at 37 °C for 3 h.

a similar direction to that of the above striations. As the attack takes place, the width of the cracks increases and when degradation is in an advanced stage, crystals become irregular since the initial edges have disappeared. However, some residual particles can remain, allowing the original crystal form to be envisaged. {010} Sectors also appear clearly degraded starting from the crystal edges although no cracks can be detected. Two interesting features should be emphasized: (a) the remaining fragments have a similar thickness to that of the crystals before degradation, as can be deduced from shadowing, (b) no holes isolated from the borders can be observed inside the exposed lamellae. Both observations seem to suggest that the degradation process started at the lateral edges of the crystals. This is in contrast with the reported data for the related polyester 6 6, which indicate that some surface attack also occurs when this polymer is exposed to the same enzyme [16]. Defects on lamellar crystal surfaces have been claimed as a possible element facilitating a hydrolysis process that gives

rise to an initial hole that rapidly becomes bigger by the action of the enzyme [7]. However, the straight cracks observed in the initial degradation stages of polyester 6 4 suggest that disordered chain-packed regions may exist inside the lamellar crystals, as has also been claimed in enzymatic degradation studies of polycaprolactone [33]. This kind of defects plays an important role in the biodegradability of the material since it is well known that the rate of degradation is controlled by the crystallinity of the material.

Polyester 6 4 can also degrade when exposed to other lipases such as *P. cepacia* (Fig. 5(b)) although in this case the process takes place more slowly. It is again clear that degradation is initiated at the chain-packing regions of single crystals rather than on the chain folding surfaces despite a homogeneous distribution of enzyme molecules on the chain-folding surfaces that can be expected from the experimental procedure. Although minimal differences can be found, the {010} growth faces appear slightly more serrated than the {110} faces, a feature that can be associated with the different packing characteristics of the corresponding sectors.

3.3. Unit cell determination

X-ray diffraction patterns of annealed fibers have a high degree of orientation, as shown in Fig. 6. Reflections extend over more than six layer lines and seem to reveal some structural disorder along the chain axis. The weak streaks that are mainly observed in the first and third layer lines must be highlighted. The patterns can be reasonably indexed assuming a monoclinic unit cell with parameters: $a = 1.604$ nm, $b = 0.732$ nm, $c = 1.440$ nm and $\beta = 38.9°$. However, it must be noted that the reflection observed at 0.769 nm could not be well indexed with the indicated unit cell. The closest spacing (0.756 nm) corresponds to the 201 reflection, but it clearly deviates from the experimental value. This problem can be solved by using a larger unit cell with a double value for the b parameter (Table 1), which in addition can justify the observed streak trend due to the great number of reflections with a moderate intensity that would appear. Note also that, as shown in the inset of Fig. 6, the reflection centered at 0.903 nm seems to be the overlapping of two very close and intense reflections (111 and 001). A cell with similar a and b dimensions has

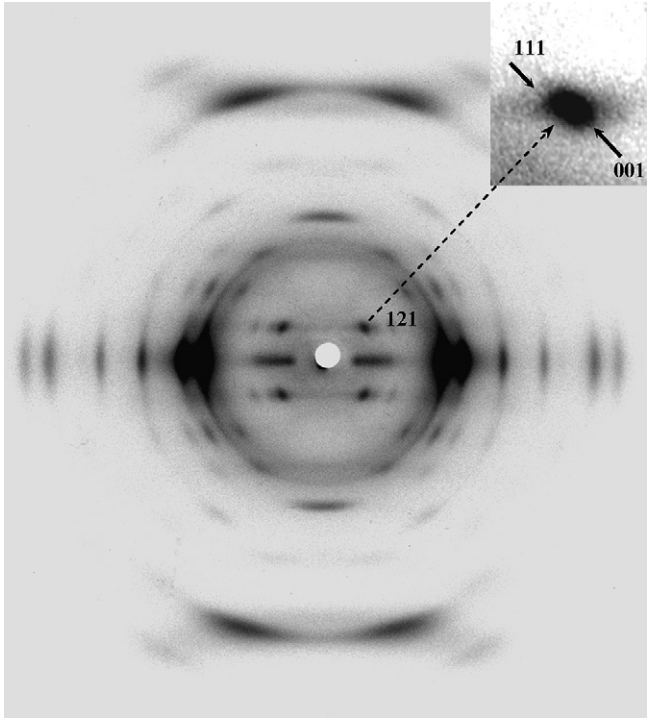

Fig. 6. X-ray fiber diffraction pattern of polyester 6 4. Inset shows a magnification of the spot corresponding to the 111 and 001 reflections. The latter defines the c^* axis.

Table 1
Calculated and measured electron and X-ray diffraction spacings d (nm) for polyester 6 4

Index[a]	Polyester 6 4		
	d_{calc} (nm)	d_{measd}[b,c] (nm)	d_{measd}[b,d] (nm)
220	0.415	0.415 vs E	0.415 vs
040	0.366	0.366 vs E	0.366 vs
240	0.296	0.296 s E	0.296 m
400	0.252	0.252 s E	0.252 s
420	0.238	0.238 vw E	0.238 w
260	0.220	0.220 s E	0.220 s
440	0.207	0.207 m E	0.207 m
080	0.183		0.183 w
460	0.175		0.175 vw
280	0.172		0.172 vw
620	0.163		0.163 w
640	0.152		0.152 vw
480	0.148		0.148 vw
101	1.420	1.415 m M	
111, 001	1.018, 0.898	0.903 vs off M	
011	0.765	0.769 m off M	
121	0.650	0.647 m off M	
303	0.472	0.472 m M	
203	0.460	0.461 m M	
002	0.449	0.453 s off M	
323	0.397	0.399 s off M	
402	0.380	0.379 s off M	
404	0.354	0.354 s M	
333	0.339	0.339 w off M	
422	0.337	0.337 w off M	
224	0.291	0.289 vw off M	
042	0.284	0.288 w off M	
405	0.286	0.283 w M	
305	0.268	0.269 w off M	
124, 624	0.252	0.250 vw off M	
543	0.240	0.242 w off M	
262	0.231	0.232 vw off M	
416	0.227	0.227 m M	
545	0.224	0.222 vw off M	
306	0.211	0.212 s off M	
464	0.201	0.203 vw off M	
336	0.194	0.195 w off M	
356	0.171	0.172 vw off M	

[a] On the basis of monoclinic unit cell with parameters $a = 1.612$ nm, $b = 1.464$ nm, $c = 1.440$ nm and $\beta = 38.6°$.
[b] Abbreviations denote relative intensities and orientations: vs, very strong; s, strong; m, medium; w, weak; vw, very weak; M, meridional; E, equatorial; off M, off meridional.
[c] X-ray diffraction data.
[d] Electron diffraction data.

recently been postulated for the related polyester 6 6 [16]. It should also be pointed out that other polyesters derived from 1,6-hexanediol [15] crystallize according to a large unit cell with a *b* parameter close to 1.49 nm.

Some features can also be explicitly indicated.

1. Reflections with strong intensity and a quasi-meridional orientation are only observed in the fourth layer line only ($l = 4$). The lack of this kind of reflections in the lower layers suggests a monoclinic unit cell, which is confirmed by the very strong (0.903 nm) and strong (0.453 nm) off meridional reflections that can be observed in the first and second layer lines, respectively. These reflections define a c^* axis that appears at an angle close to 51° with respect to the meridional *c*-axis.
2. The chain axis parameter is close to the expected value for an all-*trans* conformation (1.46 nm). However, the lower value suggests a slight distortion of the molecular conformation.
3. Equatorial reflections (as observed in the *hk*0 electron diffraction pattern) can be well indexed assuming a conventional polyester unit cell (*a* and *b* parameters of the projected rectangular unit cell close to 0.50 and 0.73 nm, respectively). However, the *a* parameter must be doubled (in chain axis projection) in order to index all the non-equatorial reflections. In this sense, the reflection observed at 0.472 nm is highly significant.

In order to confirm the indicated unit cell dimensions, we tried to obtain additional *hkl* electron diffraction data from single crystals by tilting the lamellae approximately 30° around the b^* axis. Patterns (Fig. 7) show the characteristic 0*k*0 reflections in the equator (with even *k* values) and also three layers with new reflections corresponding to the 1*k*1, 2*k*2 and 3*k*3

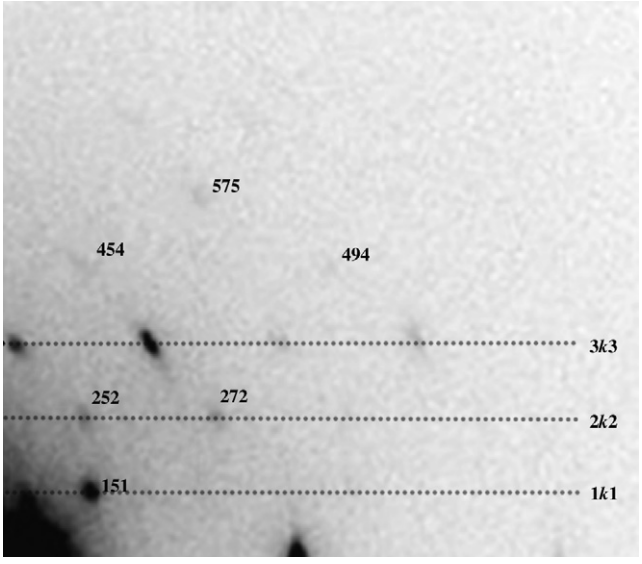

Fig. 7. Electron diffraction pattern of a polyester 6 4 lamellar crystal tilted approximately 30° around the b^* axis. Only one zone of the diffraction pattern is shown in order to enhance the labeled reflections with an odd *k* index, which are indicative of a large unit cell with a *b* parameter of 1.464 nm.

Table 2
Calculated and measured tilted electron diffraction spacings *d* (nm) for polyester 6 4

Index[a]	Polyester 6 4	
	d_{calc} (nm)	d_{measd}[b] (nm)
131	0.461	0.461 vs off M
151	0.287	0.290 vs off M
232	0.402	0.403 vs off M
252	0.271	0.275 m off M
272	0.201	0.203 m off M
323	0.397	0.387 vs off M
343	0.289	0.290 s off M
363	0.217	0.217 vs off M
383	0.171	0.171 w off M
3103	0.140	0.140 m off M
454	0.226	0.225 vw off M
494	0.148	0.148 vw off M
575	0.168	0.168 w off M

[a] On the basis of monoclinic unit cell with parameters $a = 1.612$ nm, $b = 1.464$ nm, $c = 1.440$ nm and $\beta = 38.6°$.

[b] Abbreviations denote relative intensities and orientations: vs, very strong; s, strong; m, medium; w, weak; vw, very weak; M, meridional; E, equatorial; off M, off meridional.

indices (Table 2). All reflections with odd *k* values are again highly significant since they are the main evidence of the existence of a larger unit cell with a parameter *b* equal to 1.464 nm.

The measured density of the fiber (1.17 g/mL) is fairly close to the value calculated (1.25 g/mL) from the deduced cell dimensions and a cell content of eight chain segments. Furthermore, some amorphous content exists, in agreement with the slightly lower experimental density.

3.4. Molecular packing simulation

Molecular simulation was tentatively carried out assuming a practically all-*trans* molecular conformation due to the small shortening deduced from the X-ray diffraction patterns. This conformation is compatible with a 2/*m* molecular symmetry with inversion centers in the middle of both the diol and the dicarboxylic acid units, and binary axes passing through them. The mirror plane and the binary axis symmetry should be logically lost when torsional angles deviate from 180°.

The setting angle of the molecular chains was refined taking into account the experimental intensities of the *hk*0 electron diffraction patterns. Furthermore, simulation was facilitated by considering that the chain axis projection of the structure could be well defined by a small rectangular unit cell ($a = 0.503$ nm, $b = 0.732$ nm) containing only two molecular segments (Fig. 8). Systematic absences (*h*00 and 0*k*0 with *k* and *h* odd) were detected in the electron diffraction pattern (Fig. 9(a)) when this small unit cell was considered. Thus, both chain segments could be related by glide planes or binary screw axes parallel to the *a*- and *b*-crystallographic axis.

Both the rotation angle around the fiber axis, defined as τ in Fig. 8, and the temperature factor, were the variables considered at this stage. The angle was varied at short intervals of 1° from 0° to 90°. The best fit corresponded to an *R* factor

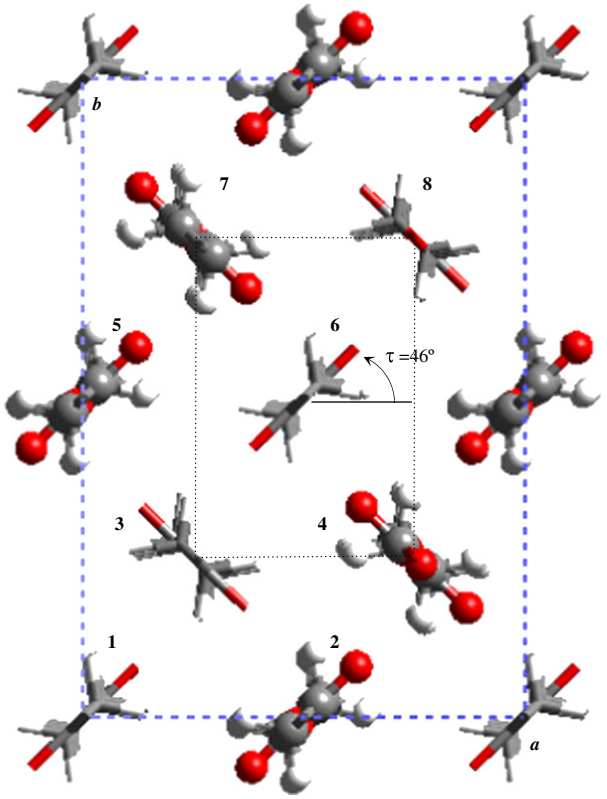

Fig. 8. View parallel to the *c*-axis direction showing the packing of polyester 6 4 assuming a large unit cell with *a* and *b* parameters of 1.612 nm and 1.464 nm, respectively. In projection this packing can be defined by a conventional rectangular cell containing only two chain segments (dotted lines). The τ setting angle used to define molecular orientation is indicated. Note that the two chain segments are related by two-fold screw axes that are parallel to the *a* and *b* directions. Chains with setting angles of ±46° are represented by sticks whereas those with setting angles of ±226° are represented by balls and sticks.

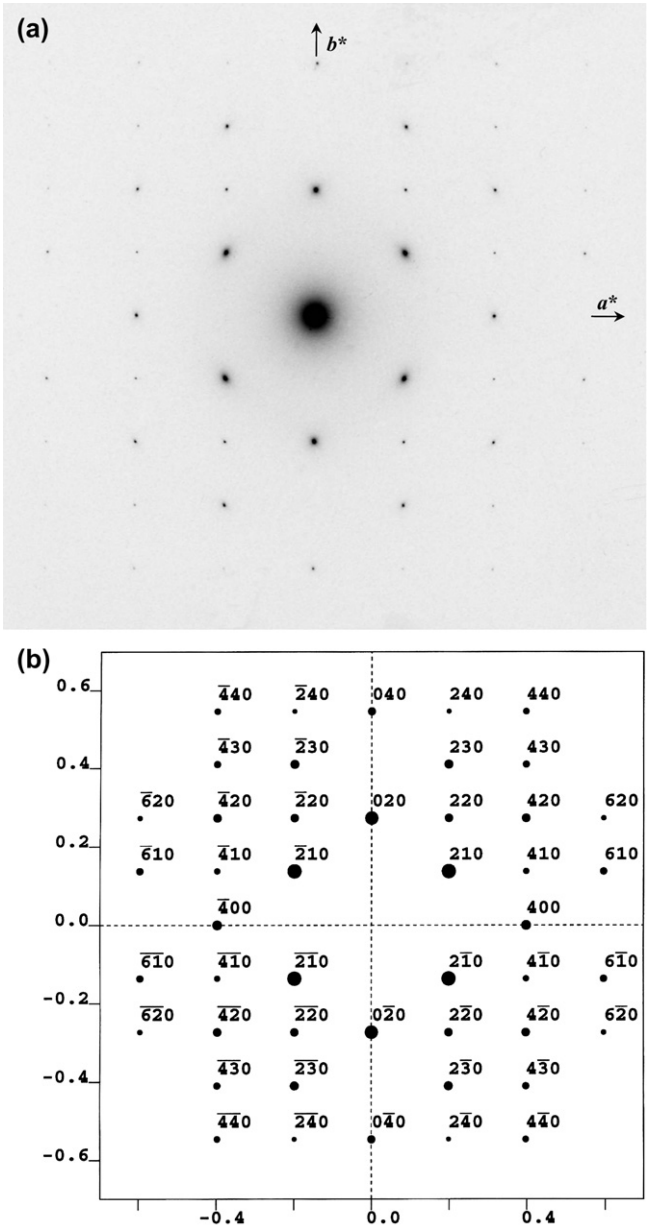

Fig. 9. Experimental (a) and simulated (b) *hk*0 electron diffraction patterns of polyester 6 4. The refined molecular packing corresponds to a setting angle of ±46°.

of 0.09 that was attained with a τ angle of 46°. A variation of ±16° for the setting angle yielded a value greater than 0.16 for this figure of merit. No improvement was obtained by considering isotropic thermal factors. Thus, the *R* factor increased up to 0.19 when a temperature factor of 5 Å^2 was considered while the setting angle was kept at the optimum value. Table 3 shows the observed and calculated structure factors, whereas Fig. 9(b) displays the electron diffraction pattern simulated with the Cerius^2 program for the optimized conditions. Both the applied procedure and the final packing characteristics are similar to those described for the related polyester 6 6 [16].

A $P\bar{1}$ space group was assumed for the crystalline structure of polyester 6 4 in order to keep the inversion center that is characteristic of molecular symmetry. Although a monoclinic unit cell is deduced from the cell dimensions, the symmetry of the space group must be reduced to the indicated inversion center. Note that the large unit cell (Fig. 8) precludes the existence of other symmetry elements that are characteristic of monoclinic space groups. For example, a binary screw axis parallel to the *b*-crystallographic axis is incompatible with the *b*/4 shift along the *b*-axis between the related chains (e.g. chains 3 and 6).

Neighbouring chains along both the *a*- and *b*-axis were assumed to have setting angles that differed by 180° in order to justify their identical chain axis projection deduced from the *hk*0 electron diffraction data, and the large unit cell deduced from X-ray and *hkl* ($l \neq 0$) electron diffraction data.

In a second stage, we simulated the X-ray fiber diffraction pattern considering the monoclinic unit cell containing eight chain segments and the $P\bar{1}$ space group symmetry. Setting angles were fixed at the deduced values, and consequently only the chain axis shifts were refined. Note that the positions of molecules 1, 2, 5 and 6 (Fig. 8) are practically defined since only two arrangements are possible for each molecule: those where the middle of their diol or dicarboxylic units coincides with the inversion center placed at a *z* fractional coordinate of 0. In this way, only the shifts of molecules 3 and 4 were systematically varied once the position of the above-mentioned

Table 3
Observed (F_0) and calculated (F_c) electron beam structure factors for polyester 6 4

h	k	l	d(obs) (nm)[a]	m[b]	F_o[c]	F_c ($\tau = 30°$)	F_c ($\tau = 46°$)			F_c ($\tau = 62°$)
						$B^d = 0$	$B^d = 0$	$B^d = 5$	$B^d = 10$	$B^d = 0$
2	1	0	0.415	2	43.41	45.79	43.41	40.36	37.53	40.86
0	2	0	0.366	1	41.77	30.15	37.41	34.08	31.04	44.95
4	0	0	0.252	1	21.26	26.85	19.50	16.01	13.14	12.64
2	3	0	0.220	2	20.15	12.02	16.65	12.84	9.91	21.45
4	2	0	0.207	2	16.27	17.94	15.06	11.26	8.42	12.07
2	2	0	0.296	2	14.99	12.11	14.48	12.55	10.88	12.19
0	4	0	0.183	1	13.51	8.76	13.63	9.39	6.46	16.81
6	1	0	0.163	2	11.22	14.75	10.86	6.80	4.26	7.04
4	1	0	0.238	2	10.41	7.68	7.87	6.31	5.06	6.57
4	3	0	0.175	2	8.55	7.87	10.44	6.95	4.62	7.35
4	4	0	0.148	2	7.60	5.79	8.61	4.87	2.75	10.70
6	2	0	0.152	2	6.72	5.23	5.70	3.33	1.94	6.40
2	4	0	0.171	2	6.06	5.68	4.68	3.07	2.01	4.45
						$R^e = 0.20$	$R^e = 0.09$	$R^e = 0.19$	$R^e = 0.29$	$R^e = 0.16$

[a] On the basis of rectangular unit cell with $a = 0.503$ nm and $b = 0.732$ nm.
[b] Multiplicity.
[c] All equivalent spots have a similar intensity.
[d] Temperature factor in $Å^2$.
[e] R factor calculated as $\sum m \cdot |F_0 - F_c| / \sum m \cdot F_0$. In each case the F_0 was escalated in order to minimize the difference between calculated and observed structure factors.

two chains was chosen in order to qualitatively fit the experimental X-ray fiber diffraction pattern to that simulated by the Cerius[2] program. Note that the setting angle of molecule 3 could be either 46 or 226°, a feature that was also considered in the refinement process. The z fractional coordinate of a representative oxygen atom of a diol unit was used to define the axial shift of molecules 3 and 4, and the position of the remaining chains (7 and 8) was fixed by the space group symmetry. The best pattern (Fig. 10) was obtained when these fractional coordinates were 0.35 and 0.45 (Fig. 11), whereas the middle of the dicarboxylic unit of molecules 1 and 2 coincided with the inversion center elements of the unit cell (placed at $z = 0$) as well as the middle of the dicarboxylic unit of molecules 5 and 6. The simulated pattern is in reasonable agreement with the experimental one although the higher spacing reflections of the second layer line do not entirely fit. However, it should be pointed out that the main trends of the first, third, fourth and sixth layers were all well reproduced. In particular, the 111 and 001 reflections appear with a high intensity, which justifies the observed strong spot corresponding to their overlapping.

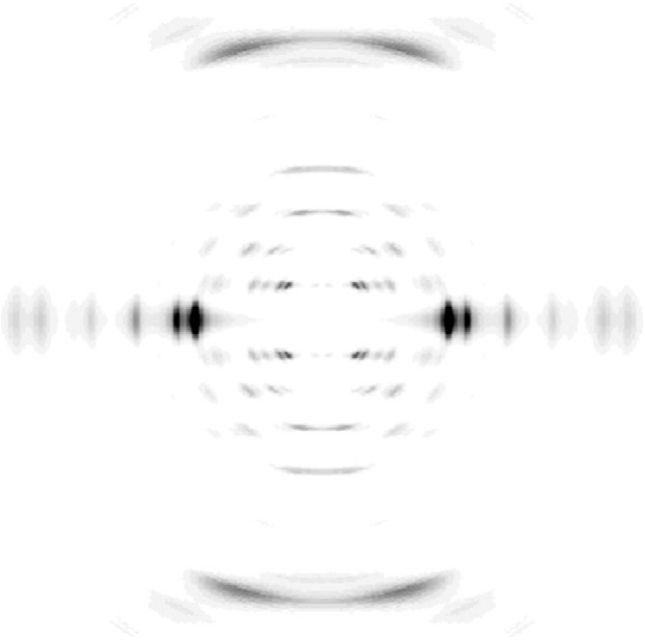

Fig. 10. Simulated X-ray fiber diffraction pattern of the refined structure of polyester 6 4 assuming a large unit cell with b parameter of 1.464 nm.

The final structure shows an alignment between the CH_2—O methylene groups and the CH_2—O oxygen atom of the diol unit, which corresponds to the most electrostatically positive groups and the most electrostatically negative atoms, respectively. Similar molecular arrangements have recently been postulated for polyesters 6 6 [16] and 6 12 [15].

4. Conclusions

Polyester 6 4 crystallizes according to a large monoclinicic unit cell of dimensions $a = 1.612$ nm, $b = 1.464$ nm, $c = 1.440$ nm and $\beta = 38.6°$. A quasi all-*trans* molecular conformation and a peculiar packing involving eight molecular segments in the unit cell can be deduced. *hk*0 electron diffraction data indicate that the chain axis projection of the structure is defined by a small rectangular cell with similar dimensions to those reported for polyethylene. Simulation of electron diffraction patterns indicate that molecular segments have setting angles of ±46° and ±226°, and neighbouring chains along the *a*- and *b*-axis have setting angles that differ by 180°. Simulation of fiber X-ray diffraction patterns indicates a chain arrangement where CH_2—O methylene groups tend to face the oxygen atoms of the diol unit of neighbouring chains, giving rise to some favorable electrostatic interactions.

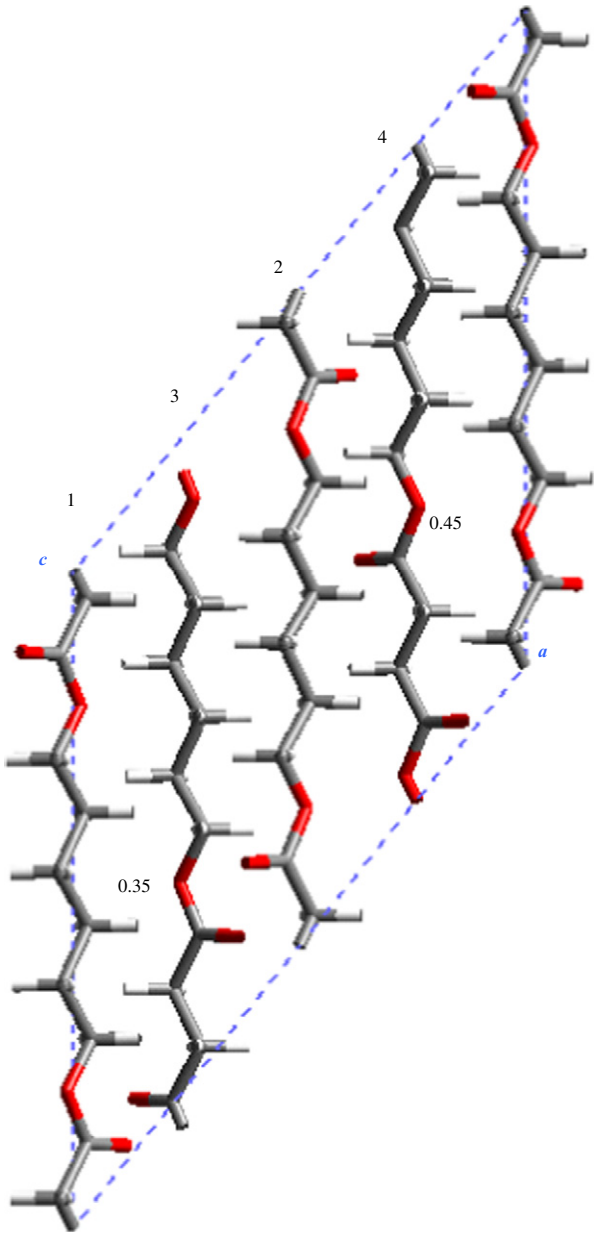

Fig. 11. View along the *b*-axis of the proposed structure of polyester 6 4. For the sake of clarity only molecules 1–4 are represented. The axial positions of molecular chains 3 and 4 are indicated by the *z* fractional coordinate of an oxygen atom of the diol unit. Color code: hydrogen, white; carbon, grey; oxygen, red (for interpretation of the references to color in this figure legend, the reader is referred to the web version of this article).

The morphology of single crystals is highly dependent on the crystallization temperature. Thus, truncated crystals with six lateral sides (four {110} and two {010} faces) are found at lower temperatures, whereas lenticular crystals with a predominant growth along the [100] direction and curved {010} faces form at higher temperatures. Decoration techniques demonstrate that the surface of lamellar crystals is ordered and that the molecular folding is parallel to the edges of the crystals in the different sectors. Crystals are also characterized by the presence of striations which form in the {110} sectors and have radial orientation or practically parallel to the [100] direction. Enzymatic degradation of single crystals with lipases mainly progresses from the crystal edges, giving rise to a fringed texture that may be correlated with the observed striations.

Acknowledgements

This research has been supported by the CICYT and FEDER (grant MAT 2006-02406). We would like to express our gratitude to Dr. Jordi Díaz of the Scientific-Technical Services of UB for the AFM micrographs.

References

[1] Scott G. Degradable polymers: principles and applications. Dordrecht: Kluwer Academic Publishers; 2003.
[2] Smith R. Biodegradable polymers for industrial applications. Cambridge: Woodhead Publishing Ltd; 2005.
[3] Doi Y, Steinbüchel A. Polyesters II – properties and chemical synthesis. New York: Wiley-VCH; 2002.
[4] Huang SJ. Encyclopedia of polymer science and engineering, vol. 2. New York: Wiley-Interscience; 1985. p. 20.
[5] Vert M. Biomacromolecules 2005;6:538–46.
[6] Takiyama E, Fujimaki T. In: Doi Y, Fukuda K, editors. Biodegradable plastics and polymers. New York: Elsevier Science; 1994. p. 150.
[7] Gan Z, Abe H, Doi Y. Biomacromolecules 2000;1:713–20.
[8] Lai SM, Huang CK, Shen HF. J Appl Polym Sci 2005;97:257–64.
[9] Fujimaki T. Polym Degrad Stab 1998;59:209–14.
[10] Ueda AS, Chatani Y, Tadokoro H. Polym J 1971;2:387–97.
[11] Aylwin PA, Boyd RH. Polymer 1984;25:323–9.
[12] Liau WB, Boyd RH. Macromolecules 1990;23:1531–9.
[13] Kanamoto T, Tanaka K. J Polym Sci Part B Polym Phys 1971;9:2043–60.
[14] Almontassir A, Gestí S, Franco L, Puiggalí J. Macromolecules 2004;37:5300–9.
[15] Gestí S, Almontassir A, Casas MT, Puiggalí J. Polymer 2004;45:8845–61.
[16] Gestí S, Almontassir A, Casas MT, Puiggali J. Biomacromolecules 2006;7:799–808.
[17] Wittmann JC, Lotz B. J Polym Sci Part B Polym Phys 1985;23:205–26.
[18] Zou XD, Sukharev Y, Hovmöller S. Ultramicroscopy 1993;49:147–58.
[19] *Cerius*^{2}. Accelrys Inc., Cambridge, UK; 2002.
[20] Toda A. In: Dosiere M, editor. Crystallization of polymers. Dordrecht/Boston/London: Kluwer Academic Publishers; 1993. p. 141–52.
[21] Keller A. Philos Mag 1957;2:1171–5.
[22] Fischer EW. Z Naturforsch 1957;12a:753–5.
[23] Till PH. J Polym Sci 1957;24:301–5.
[24] Keith HD. J Appl Phys 1964;35:3115–26.
[25] Sadler DM. Polymer 1983;24:1401–9.
[26] Mansfield ML. Polymer 1988;29:1755–60.
[27] Toda A. Polymer 1991;32:771–80.
[28] Point JJ, Villers D. J Cryst Growth 1991;114:228–38.
[29] Frank FC. J Cryst Growth 1974;22:233–6.
[30] Keller A. Kolloid Z Z Polym 1967;219:118–31.
[31] Pouget E, Almontassir A, Casas MT, Puiggalí J. Macromolecules 2003;36:698–705.
[32] Furuhashi Y, Iwata T, Sikorski P, Atkins E, Doi Y. Macromolecules 2000;33:9423–31.
[33] Iwata T, Doi Y. Polym Int 2002;51:852–8.
[34] Navarro E, Alemán C, Subirana JA, Puiggalí J. Macromolecules 1996;29:5406–15.
[35] Hocking PJ, Marchessault RH, Timmins MR, Lenz RW, Fuller RC. Macromolecules 1996;29:8330–3.